A Special Refereed Issue (Volume 19) – Selected articles from the International Engineering Technologies and Applied Sciences Conference and Exhibition, Baghdad, Iraq, 2024

https://doi.org/10.14525/JJCE.v19i5.02

Jordan Journal of Civil Engineering

Journal homepage: https://jjce.just.edu.jo

Dynamic Loading Effects on a Flexible Pavement Reinforced with Geotextile

Omaima A. Menkash [1)*], ***Hasan H. Joni*** [2)], ***Maha H. Nsaif*** [3)]

[1)] *Master Student, Corresponding Author. Email: bce.22.53@grad.uotechnology.edu.iq*
[2)] *Professor. Email: 40317@uotechnology.edu.iq*
[3)] *Lecturer. Email: 40273@uotechnology.edu.iq*
[1),2),3)] *Civil Engineering Department, University of Technology, Iraq.*

Pages: 10 - 18

Published: August, 2025

ABSTRACT

When exposed to static and dynamic traffic loading, road pavements can exhibit degradation and permanent surface deformation. This study examined the impact of dynamic loading on the layers of a flexible pavement. This study used two types of geotextile (woven and non-woven) as reinforcements. Two cases were investigated; the first one by placing the reinforcement within the wearing layer, and the other one by placing it between the wearing and base layers. The road layers experienced a harmonic dynamic load with an amplitude of 1.5 tons and a frequency of 0.25 Hz. The measurement of strain in the layers of the road was carried out using a strain gauge sensor. The results indicated that when geotextile was placed between the wearing and base layers, it provided a better reinforcement with a reduction of 74.8% in strain using woven geotextile.

Keywords: Geotextile reinforcement, Flexible pavement, Sliding between layers, Strain, Strain gauge sensor, Dynamic load.

INTRODUCTION

One of the main elements influencing road life and service capacity and potentially causing damage to the road is the dynamic load of the vehicle (Watts & Krylov, 2000; Pan & Li, 2002). Geosynthetics are used in pavement construction for a number of applications, such as foundation reinforcement, asphalt reinforcement, sub-grade stability, drainage, and filtration (Mohammed et al., 2016; Al-Obaidi et al., 2022; Ansari and Roy, 2023). Several scenarios of extensive trials were completed in Thailand. The efficacy of geosynthetics in strengthening flexible pavements was examined. Four experimental segments were used to observe the structural behavior. Geosynthetics were inserted into the pavement at different depths. The findings indicated that each reinforcement method caused a decrease in both the static and dynamic loads produced at the pavement base (Imjai et al. 2019). Wang et al. (2020) utilized geocells, geotextiles, and geogrids, which are commonly exploited as geosynthetic materials in pavement applications. This is because they are quite successful in attaining favorable results. Jebur et al. (2021) designed a laboratory model to comprehend how dynamic loading affects the base layer and the flexible pavement. The reinforcement is applied at the base-sub-grade interface using the SS2 type of geogrid. The load applied to the road layers was dynamic and harmonic, with load magnitudes of ten kilometers and fifteen kilonewtons,

and with 0.5 Hz and 1.0 Hz frequencies, respectively. The results showed that by using a geogrid between the sub-grade and base layer, the vertical displacement and stress decreased, especially under higher loads and frequencies. Hussein (2021) examined the performance of pavement layers during simulated earthquake conditions. In this investigation, the layers underwent experimental testing while being exposed to earthquake loads at several frequencies, including 0.5, 1, and 1.5 Hz. The tests comprise two components: one without the geogrid and the other with the geogrid placed in the middle of the base course and between the base course and the sand course. The stress gauge sensors were employed to monitor the applied stresses in the three layers, whilst the displacement gauge sensor was utilized to measure the movements of the surface layer. The results obtained suggest that the models enhanced with geogrid demonstrate elevated levels of stress in comparison to the models without reinforcement. Nevertheless, displacement decreased as the number of geogrid layers grew at the three distinct frequencies.

Al Sa'adi et al. (2022) utilized geotextile reinforcement in many layers to assess the effectiveness of asphalt pavement in preventing rutting failures. The study found that using geotextiles effectively decreases the formation of ruts in flexible pavement. Menkash et al. (2024) investigated the utilization of geotextile within the asphalt layer to prevent sliding. A four-point bending test was conducted. Three distinct amounts of micro-strain (250, 400, and 750) were delivered. The results indicated that combinations lacking reinforcement had a decreased fatigue lifespan compared to surface layers fortified with geotextile. Moreover, when exposed to various temperatures (5°C, 20°C, and 30°C), it was noticed that the geotextile inter-layer system exhibited reduced effectiveness in cold conditions compared to warm and moderate climates.

Through reviewing earlier research that involved improvement of the pavement, this research uses two types of geotextile as a kind of reinforcement. Woven geotextiles and non-woven geotextiles were used as reinforcement between the surface and the base course and in the middle of the wearing course pavement to improve the performance of the pavement.

Materials, Asphalt Slab Preparation, and Test Procedures

Materials employed in this study include asphalt cement, aggregate, mineral filler, and geotextile. Below is a description of the materials that were used.

Asphalt Cement (AC): AC utilized in this study was supplied by the Dura refinery in Baghdad with a penetration grade of (40-50). The penetration grade selected for this investigation is appropriate for high-temperature areas with excessive summer softening, resistance to heavy traffic loads, and standard compliance. Table 1 lists the asphalt binder's physical characteristics.

Table 1. Physical characteristics of AC

Property	ASTM method	Unit	Test results	SCRB specification
Penetration at 25˚C, 100gm , 5 sec	D5	0.1 mm	47	40-50
Ductility at 25˚C, 5cm/min	D113-99	cm	139	>100
Flash point (Cleveland open cup)	D92	˚C	324	Min. 232
Softening point	D36	˚C	53	-------
Specific gravity at 25˚C	D70	-------	1.05	-------
Viscosity at 135˚C	D-4402	c.p	613	-------
Viscosity at 165˚C	D-4402	c.p	156	-------

Aggregate: AL-Nibaie quarry north of Baghdad provided the aggregate for this project. The surface-course and base-course aggregate shall adhere to the maximum size specified in the State Corporation of Roads and Bridges SCRB R/9, 2003. Table (2 and Figures 1 and 2 display the aggregate properties, gradation for the wearing course, and gradation for the base course, respectively.

Mineral Filler: In this investigation, limestone was used as the mineral filler. Table 3 lists the physical characteristics of limestone dust.

Table 2. Physical characteristics of aggregate

Property	Value	ASTM designation
Coarse Aggregate		
Bulk specific gravity	2.628	C127
Water absorption%	0.94	C127
Toughness % (Los Angeles abrasion)	20.2%	C131
Fine Aggregate		
Bulk specific gravity	2.569	C128
Water absorption%	0.92	C128

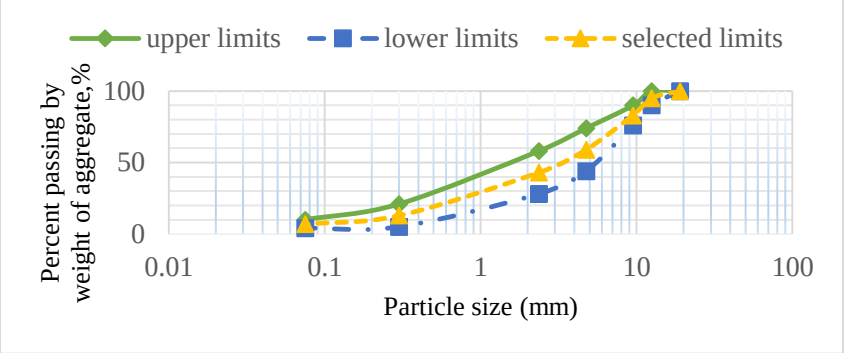

Figure 1. Gradation curves of the aggregate for wearing course

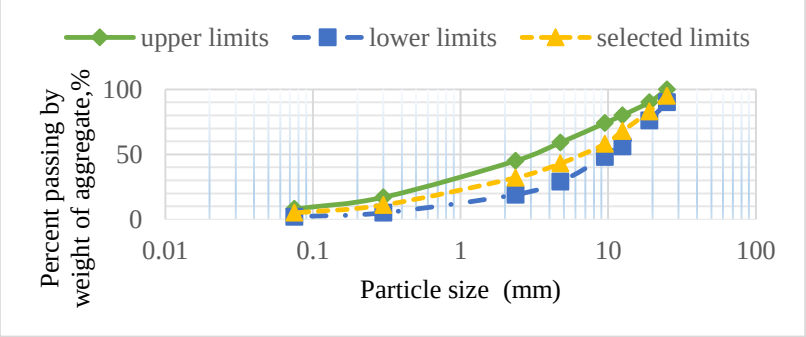

Figure 2. Grain size distribution curve of base course

Table 3. Physical characteristics of limestone dust

Property	Results
Specific gravity	2.77
Passing sieve no. 200 (0.075mm)	94 %

Geotextile: In this study, two types of geotextile were used which were obtained from a commercial company: The first type is woven geotextile, as depicted in Figure 3 and Table 4. The second type is non-woven geotextile, as depicted in Figure 4 and Table 5. Chinese manufacturer (which attached a certificate for the properties of the material mentioned in the tables).

Figure 3. Woven geotextile reinforcement

Marshall Mix Design Method: Marshall mix design approach was employed to determine the optimum binder content for two layers; the recommended asphalt contents were determined to be 4.9% and 3.5% for the surface course and the base course, respectively. The surface course needs a higher asphalt content for durability, moisture resistance, and flexibility against

cracking, while the base course needs a lower asphalt content to ensure strength and structural support for the pavement. This is why the two layers have different asphalt contents (4.9% for the surface course and 3.5% for the base course).

Table 4. Physical, dimensional and mechanical properties of woven geotextile

Physical properties		
Property	**Value**	
Mesh type	Diamond	
Standard color	Green	
Polymer type	High density polyethylene (HDPE)	
Dimensional properties		
Property	**Unit**	**Value**
Aperture size	mm	12 × 15
Mass per unit area	g/m²	283
Thickness	mm	1.2
Mechanical properties		
Tensile strength	kN/m	60
Elongation at max load	%	22.7

Figure 4. Non-woven geotextile reinforcement

Preparation of Asphalt Slab: To create the required asphalt slab, a steel mold measuring 30cm × 30cm × 5cm was employed to prepare the wearing coarse layer, while another mold measuring 30cm × 30cm × 10cm was utilized for the base course. These asphaltic mixes were subjected to short-term aging by being placed at 135°C for 4 hrs according to AASHTO PP2. An asphalt mixture was compressed using a compression machine. After twenty-four hours, the slab was emitted from the mold and then subsequently coated with polyethylene to protect it from the surrounding environment.

Dynamic Load Test: A dynamic loading mechanism was used to replicate the dynamic load placed on pavement layers in the laboratory. This apparatus was first designed by Abd Al-Kareem (2013) at the University of Technology/Iraq. The device employed was an electric air compressor with a maximum load amplitude of 12 kN. The device adjustment was created by raising the loading amplitude to (60 kN) (Aswad, 2016). This tool is made up of the following components: I. a loading frame made of steel. II. a system of hydraulic loading. III. model footing. IV. a data acquisition and logging system. V. a steel container. VI. a data logger system and strain gauge underneath the asphalt model, as shown in Figure (5).

Figure 5. General view of the loading system

Table 5. Properties of non-woven geotextile

Physical properties		
Property	Unit	Result
Mass per unit area (EN ISO 9864)	g/m²	200
Thickness (EN ISO 9863)	mm	1.30
Mechanical properties		
Tensile strength in the machine direction MD (EN ISO 10319) cross-machine direction CMD	kN/m	16
Elongation at max load MD (EN ISO 10319) CMD	%	60-65
Hydraulic properties		
In-plane flow capacity (EN ISO 12958)	10^{-3} l/ms	2.1
Characteristic opening size (EN ISO 12956)	μm	80

Unreinforced Models: The test was conducted in a 500 mm × 500 mm × 500 mm-height well-tied steel box surrounded by cork to stop waves from reflecting during the test. Clean and dried sub-grade dirt is placed within the box. After that, the dry dirt is gathered and manually combined with 16% of the required water, the quantity of water required to achieve the material's optimal moisture content (OMC), which guarantees the highest compaction and performance. Also, its California Bearing Ratio (CBR) is 45. Subsequently, the sub-grade is placed inside the steel box and compacted into three levels, each 20 cm thick. After that, the base layer with a thickness of 10 cm was positioned on top of the sub-grade. Then, its wearing layer thickness is 5 cm and the sensor is placed at the bottom of the asphalt model.

Reinforced Models: The prepared soil was covered with a base layer. The base layer was then covered with a layer of woven geotextile. The base course layer is subsequently covered by the asphalt slab (wearing layer). The procedures are then repeated with the non-woven geotextile. The other case, which applies to both kinds, places the geotextile within the surface layer.

RESULTS AND DISCUSSION

Strain Findings (Unreinforced Models): The data that appeared on the Excel sheet was displayed on the screen of the dynamic load device according to the software equations of the placed strain sensors and data logger. The strain values in the wearing layer and the base layer of a flexible pavement are depicted in Figure 6. According to the results, the strain (in micro-strains) over time (in seconds) for two pavement layers: the asphalt layer and the base layer. In the Initial Phase (0-200 seconds), the strain in the asphalt layer rises rapidly, peaking at around 400 micro-strains during the early phase. This indicates that the asphalt layer is highly responsive to the applied load, likely due to its flexible nature. The base layer strain fluctuates initially, but remains much lower compared to that of the asphalt layer. This suggests that the base layer absorbs less deformation in the early stage, likely acting as a support layer. However, in the intermediate phase (200-600 seconds) after the rapid rise, the strain in the asphalt layer shows significant fluctuations, with peaks and valleys. These fluctuations could be caused by varying load intensities or temperature effects impacting the asphalt's visco-elastic behavior. The strain in the base layer steadily increases during this period, reaching around 250 micro-strains. This reflects a gradual load transfer from the asphalt layer to the base layer, indicating stress distribution within the pavement structure. In the final phase (600-1000 seconds), the strain in the asphalt layer starts to decline after peaking at around 700 microstrains. This reduction might indicate stabilization in the layer or recovery after the cessation of dynamic loads and the strain in the base layer stabilizes, fluctuating around 150-200 microstrain. This behavior suggests that the base layer effectively supports the residual load transferred from the asphalt layer.

Strain Findings (Reinforced Models): By using woven and non-woven geotextiles amidst the wearing course layer, Figure 7 depicts the connection between strain and time and shows that when applying a load of 1.5 tons with a frequency of 0.25 Hz, it has been noticed that strain is reduced by 45.7% when using woven geotextile and by 28.6% when using non-woven geotextile for the wearing layer. Additionally, the strain decreases by 34% with the use of woven geotextile and by 26.7% with the use of non-woven geotextile for the base layer.

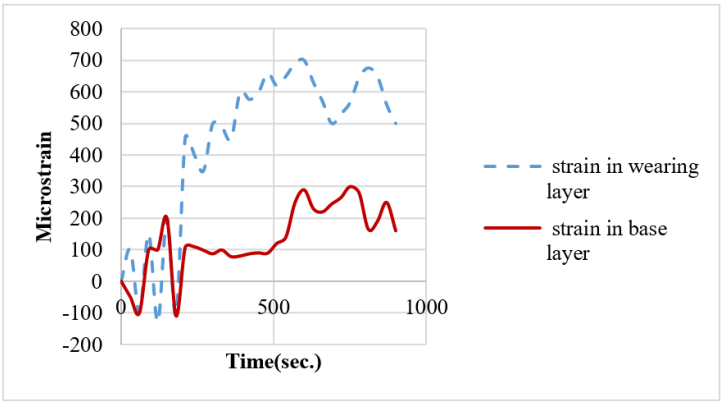

Figure 6. Strain in a flexible pavement wearing and base layers

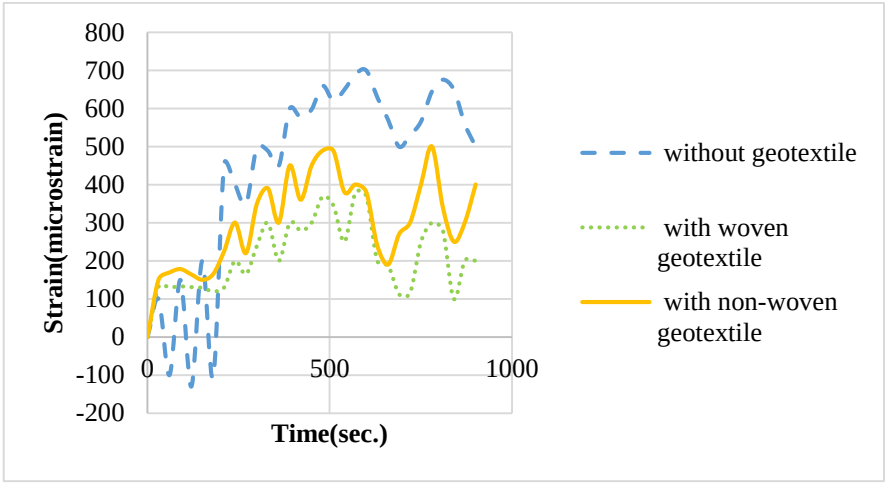

a) Strain in the wearing layer

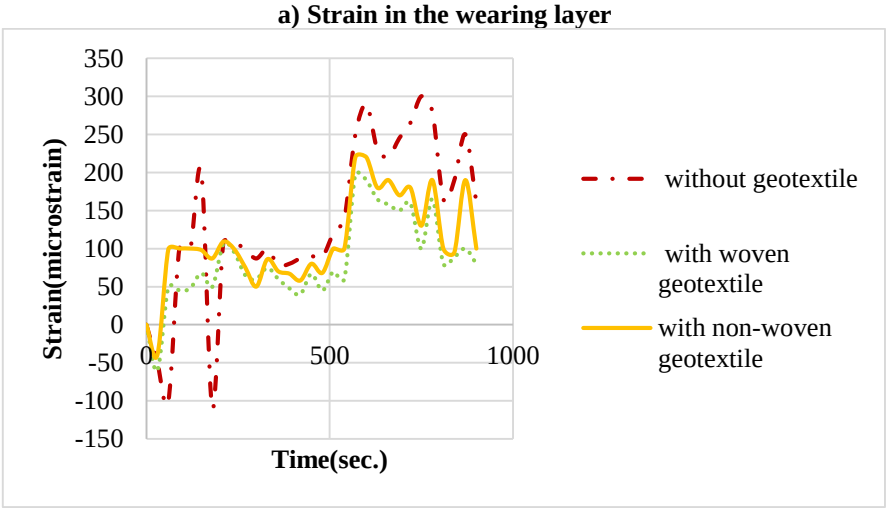

b) Strain in the base layer

Figure 7. Strain of the wearing layer and the base layer.
a) Strain of the wearing layer and b) Strain of the base layer

It can be seen that geotextile can give better interlocking, because there are openings that allow strong bonding between the asphalt layers, the mechanism of load transfer increases through the asphalt and aggregate particles leading to an increase in the load-bearing capacity to spread the loads across the reinforced foundation and into the lower layer. Because of this, the loads exerted on the sub-grade are lessened. In addition, this prevents insulation between layers and sliding, thus reducing strain.

Strain Results for Reinforced Models: Woven and non-woven geotextiles were inserted between wearing and base layers, Figure 8 shows that the road was more efficient and the strain was reduced by 74.8% and 66.5%, respectively, when a layer of geotextile reinforcement was positioned between the wearing and base layers. Woven geotextile can lower the strain in the base layer by 61.3%, whereas non-woven geotextile can reduce it by 48%. When reinforcement is placed in the wearing layer, its ability to reduce strain values is much lower compared to when it is inserted between the wearing and base layers. The explanation of this phenomenon is that the reinforcement located at the interface between the wearing layer and the base layer provides lateral resistance due to the forces of friction and inter-locking. This reinforcement placement results in an augmentation of the membrane support for wheel loads and the failure areas of the bearing that are embedded in the pavement being analyzed, hence improving the shear strength (Kinney et al., 1998).

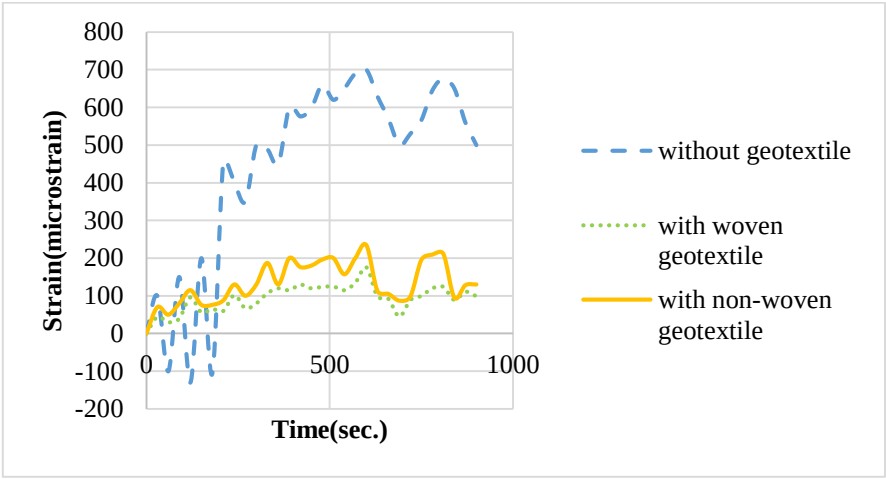

a) Strain in the wearing layer

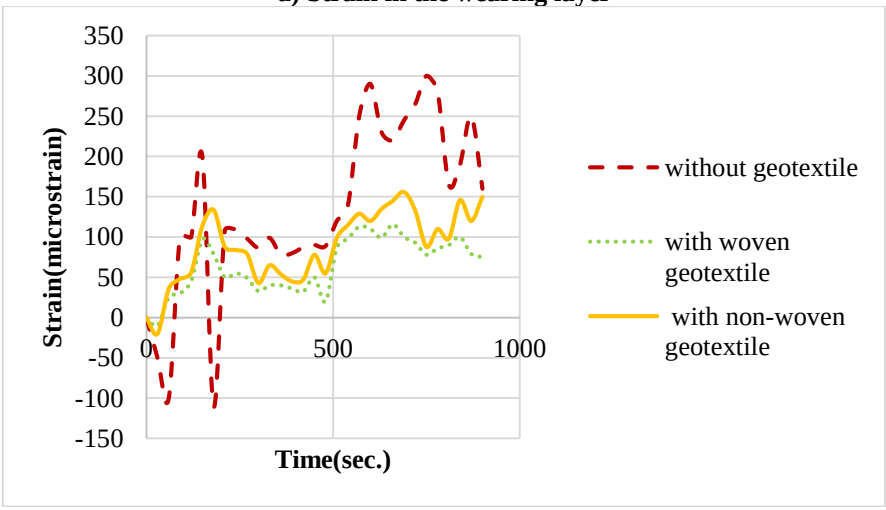

b) Strain in the base layer

Figure 8. Strain of the wearing layer and the base layer.
a) Strain of the wearing layer and b) Strain of the base layer

CONCLUSIONS

- When geotextile is located within the wearing course layer, strain decreases for the wearing layer by 45.7% using a woven geotextile and by 28.6% using a non-woven geotextile. Also, strain decreases by 34% with the use of a woven geotextile, and by 26.7% with the use of a non-woven geotextile for the base layer.
- When geotextile is placed between the base and wearing layers, a higher reduction in strain could be obtained, which is 74.8% and 66.5% by using woven and non-woven geotextiles, respectively, for the

wearing layer, and by 61.3% using a woven geotextile and 48% using a non-woven geotextile for the base layer.

- According to the results of this study, the most resistance to dynamic load was gained by placing the geotextile between the base and wearing layers, as indicated by the reduction of strain compared to the control section (without reinforcement).

REFERENCES

AASHTO-PP2. (1999). Standard practice for mixture conditioning of hot mix asphalt (HMA).

Abd Al-Kaream, K.W. (2013). *The dynamic behavior of machine foundation on saturated sand*. Master's Thesis. Civil Engineering Department, University of Technology, Baghdad.

AFNOR. (2005). *EN ISO 9864: Geosynthetics: Test method for the determination of mass per unit area of geotextiles and geotextile-related products* (5 p.). Association Française de Normalisation.

AFNOR. (2006). *EN ISO 9863-1: Geosynthetics: Determination of thickness at specified pressures-Part 1: Single layers* (In revision, 8 p).

AFNOR. (2010). *EN ISO 12956: Geotextiles and geotextile-related products: Determination of the characteristic opening size* (10 p).

AFNOR. (2010). *EN ISO 12958: Geotextiles and geotextile-related products: Determination of water flow capacity in their plane* (13 p).

Al-Obaidi, Q.A., Mohsenm M.K., & Asker, A.O. (2022). Investigation of the bearing capacity and collapsibility of gypseous soil using geotextile reinforcement. *Engineering and Technology Journal, 40*(5), 792-801. https://etj.uotechnology.edu.iq

Al Sa'adi, A.H.M., Al-Khafaji, F.F., Hashim, T.M., Hussein, M.L. A., Ali, Y.A., Ali, A.H., Jebur, Y.M., Ali, L.H., Al-Mulali, M.Z., & Al-Khazraji, A.A. (2022). Prospect of using geotextile reinforcement within flexible pavement layers to reduce the effects of rutting in the middle and southern parts of Iraq. *Journal of the Mechanical Behavior of Materials, 31*(1), 323-336. https://doi.org/10.1515/jmbm-2022-0040

Ansari, M.A., & Roy, L.B. (2023). Effect of geogrid reinforcement on shear strength characteristics of a rubber-sand mixture under undrained triaxial test. *Jordan Journal of Civil Engineering, 17*(2). https://doi.org/10.14525/JJCE.v17i2.01

ASTM International. (1992). *ASTM C 127-88: Test method for specific gravity and absorption of coarse aggregate*. Annual Book of ASTM Standards.

ASTM International. (1992). *ASTM C 128-88: Test method for specific gravity and absorption of fine aggregate*. Annual Book of ASTM Standards.

ASTM International. (1992). *ASTM D 113: Standard test method for ductility of bituminous materials*. Annual Book of ASTM Standards.

ASTM International. (1992). *ASTM D 36: Standard test method for softening point of bitumen (ring-and-ball apparatus)*. Annual Book of ASTM Standards.

ASTM International. (1992). *ASTM D 5: Standard test method for penetration of bituminous materials*. Annual Book of ASTM Standards.

ASTM International. (1992). *ASTM D 70: Standard test method for density of semi-solid bituminous materials (pycnometer method)*. Annual Book of ASTM Standards.

ASTM International. (1992). *ASTM D 92: Standard test method for flash and fire points by Cleveland open cup tester*. Annual Book of ASTM Standards.

ASTM International. (1996). *ASTM C 131-96: Standard test method for resistance to abrasion of small size coarse aggregate by use of the Los Angeles machine*. Annual Book of ASTM Standards.

ASTM International. (2015). *ASTM D 4402-2015: Standard test method for viscosity determination of asphalt at elevated temperatures using a rotational viscometer*. Annual Book of ASTM Standards. https://doi.org/10.1520/D4402

Aswad, M.F. (2016). *Behavior of improved railway ballast overlying clay using geogrid*. PhD Thesis, University of Technology.

EN ISO 10319. (2015). *Geosynthetics*: *Wide-width tensile test*. European Committee for Standardization, Brussels, Belgium.

Hussein, M.M., Eweis, M.K., & Morsy, M.M. (2021). Laparoscopic *versus* open complete mesocolic excision for right cancer colon. *Oncology in Clinical Practice, 17*(4), 148-156. https://doi.org/10.5603/OCP.2021.0025

Imjai, T., Pilakoutas, K., & Guadagnini, M. (2019). Performance of geosynthetic-reinforced flexible pavements in full-scale field trials. *Geotextiles and Geomembranes, 47*(2), 217-229. https://doi.org/10.1016/j.geotexmem.2018.12.012

Jebur, F., Fattah, M., & Abduljabbar, A. (2021). Function and application of geogrid in flexible pavement under dynamic load. *Engineering and Technology Journal*, *39*(8), 1231-1241. https://etj.uotechnology.edu.iq

Kinney, T.C., Abbott, J., & Schuler, J. (1998). Benefits of using geogrids for base reinforcement with regard to rutting. *Transportation Research Record, 1611*, 86-96. https://doi.org/10.3141/1611-11

Menkash, O.A., Joni, H.H., & Nsaif, M.H. (2024). An experimental study on the tensile properties of reinforced asphalt pavement. *Open Engineering*, *14*(1), Article 20220591. https://doi.org/10.1515/eng-2022-0591

Mohammed, Y., Aladili, A.S., & Yousif, H.F. (2016). Evaluation of reinforced sub-base layer on expansive sub-grade soil. https://doi.org/10.30684/etj.34.9A.7

Pan, Y.Z., Li, D.P., & Pan, H.L. (2002). Inhibition of glutamatergic synaptic input to spinal lamina IIo neurons by presynaptic α2-adrenergic receptors. *Journal of Neurophysiology*, *87*(4), 1938-1947. https://doi.org/10.1152/jn.00575.2001

SCRB/R9 General Specification for Roads and Bridges. (2003). *Section R/9, hot-mix asphalt concrete pavement* (Revised edn.). State Corporation of Roads and Bridges, Ministry of Housing and Construction, Republic of Iraq.

Wang, X., Zhang, X., Zhu, Y., Su, T., & Li, X. (2020). Full-scale field investigation of asphalt pavements reinforced with geocells. *Transportation Research Record*, *2675*(1), 269-279. https://doi.org/10.1177/0361198120962091

Watts, G.R., & Krylov, V.V. (2000). Ground-borne vibration generated by vehicles crossing road humps and speed control cushions. *Applied Acoustics*, *59*(3), 221-236. https://doi.org/10.1016/S0003-682X(99)00026-2.